Key Engineering Materials
ISSN: 1662-9795, Vol. 926, pp 1977-1985
doi:10.4028/p-2v2esd

Submitted: 2021-12-07
Revised: 2022-01-30
Accepted: 2022-02-03
Online: 2022-07-22

Influence of the Grain Boundary Curvature Model on Cellular Automata Static Recrystallization Simulations

Szymon Niewczas[1,a], Mateusz Sitko[1,b*] and Lukasz Madej[1,c]

[1]Faculty of Metals Engineering and Industrial Computer Science, AGH University of Science and Technology, Mickiewicza 30 av., 30-059 Krakow, Poland

[a]sniewczas@student.agh.edu.pl; [b]msitko@agh.edu.pl; [c]lmadej@agh.edu.pl

Keywords: cellular automata, static recrystallization, boundary curvatures models

Abstract. Determination of the influence of grain boundary curvature model type on the cellular automata (CA) static recrystallization (SRX) simulation predictions is the primary goal of the research. The developed CA model is a full-field approach that captures local heterogeneities in grain morphology, crystallographic orientation, and distribution of stored deformation energy. The main driving force of the model is the value of the stored energy; however, the curvature of the grain boundary may also play a role during the recrystallization. Therefore, different variants of grain boundary curvature calculations within the discrete computational domain during recrystallization and additionally subsequent grain growth are compared within this work.

Introduction

The final grain size and phase composition significantly impact the physical properties of metallic polycrystalline materials from which finished products are manufactured. Therefore, many scientific investigations focus on the experimental analysis of phenomena occurring during grain growth, recrystallization, or phase transformation [1] and, in particular, on the evaluation of grain boundaries location [2,3]. Despite the application of advanced laboratory observation techniques such as scanning electron microscope (SEM) additionally equipped with an electron backscattered diffraction (EBSD) detector [4] or using a transmission electron microscope (TEM), the detailed process of microstructure evolution during static recrystallization and grain growth is still difficult to follow precisely. Even 3D computed tomography techniques have their limitations [5]. Therefore, this type of research is intensively supported by numerical simulation methods, which provide the result in the form of a synthetic microstructure so that important material features are visualized and considered during simulation in a direct way. Examples of numerical methods that are increasingly used in such studies are, e.g., Monte-Carlo (MC) [6,7], Phase Field (PF) [8], Level Set [9] or Vertex Method (VM) [10]. Static recrystallization models based on these approaches have been successfully applied to study grain growth kinetics, grain size distribution, effect of nuclei distribution on microstructure evolution [11], or to simulate many complex processes occurring during thermo-mechanical processing [12]. The main challenge in the aforementioned numerical approaches is the link between simulation time and real-time (MC) or the relatively long computation time associated with the precise identification of the grain boundary (PF) position. In addition, some parameters needed for a given model are chosen empirically and are often not reflected in measurable values. Some of these limitations are solved by static recrystallization models developed according to the Cellular Automata (CA) method [13,14]. Like the MC model, the CA model is not perfect in simulating the grain growth process of a material, especially when experimental data for its identification are missing. However, models based on cellular automata directly calculate the grain boundary velocity while taking into account the effect of grain boundary curvature in a straightforward way (Curvature Based Cellular Automata, CB-CA). The CB-CA model has been used to simulate the material grain growth process in the following works, e.g., [15,16]. The most popular model for calculating grain boundary curvature in the cellular automata approach was presented by Kremeyer in [17]. However, in the literature, one can find other more elaborated models for calculating grain boundary curvature, e.g., Mason [18] or based on the so-called concentration gradients [15]. However, the calculated curvature values in these cases are often partially dependent on the shape of the cells in the automaton space and the selected neighbourhood type.

Therefore, this paper aims to evaluate the influence of selected grain boundary curvature models on the grain boundary behaviour during cellular automata simulation of the static recrystallization phenomenon. The grain growth phenomenon can lead to a significant rearrangement of the material morphology during annealing or after recrystallization, which results in a change of final mechanical properties. Therefore, control of this phenomenon is crucial for the practical use of such models.

SRX Model Assumptions

The CA static recrystallization model presented in the paper considers the recovery, nucleation, and subsequent growth of recrystallized grains. At the beginning of each iteration, the recovery mechanism is initiated, and the total amount of stored energy is reduced in each CA cell separately, as present in [19]. After the recovery stage, nucleation of new recrystallized grains is considered. The site saturated nucleation [20] is assumed during the current research to compare the effect of curvature on grain behaviour, but continuous nucleation is also implemented within the model. For SRX simulations, nucleation is based on a probabilistic model described by the equation:

$$P_{NUC} = C_0\left(H_i - H^c\right)\exp\left(-\frac{Q_N}{RT}\right)S_N t_{step}, \tag{1}$$

where: C_0 - nucleation parameter, H_i - energy stored in the CA cell, H^C - critical stored energy value for nucleation, Q_N - activation energy for nucleation, R - universal gas constant, T - temperature, S_N - volume in which the nucleus can appear, t_{step} - length of a time step in each CA iteration.

As recrystallized cells emerge, the CA cell growth is considered. The velocity of each i^{th} CA cell during this stage is based on the mobility and the net pressure:

$$v_i = M_G P, \tag{2}$$

where: M_G - grain boundary mobility, P - net pressure on the grain boundary [21].

In the present work, the net pressure on the grain boundaries is based on the summation of the two major driving forces associated with stored energy P_E and grain boundary curvature P_{GB} (different models of grains boundary curvature are presented in the next chapter), but it can be additionally complemented with the possible influence of precipitates P_Z [22]:

$$P = P_E + P_{GB} + P_Z, \tag{3}$$

Then, the equation (2) is considered for each CA cell which is located at the recrystallization front in t^{th} time step:

$$RX_{i,t}^{fraction} = RX_{i,t-1}^{fraction} + \sum_{j=1}^{rx}\left(\frac{v_j t_{step}}{C_S}\right), \tag{4}$$

where: $RX_{i,t-1}^{fraction}$ - recrystallization volume fraction in i^{th} CA cell in the t-1 time step, v_j – velocity of the recrystallization front in j^{th} cell from eq. (2), rx - number of recrystallized neighbours, C_S - physical cell size.

Finally, based on equation (4), transition rules are defined for the growth of subsequent recrystallized cells:

$$Y_i^{t+1} = \begin{cases} SRX \Leftrightarrow RX_{i,t}^{fraction} > 1.0 \\ Y_i^t \end{cases}, \tag{5}$$

where: SRX - cell recrystallized in the current step, Y_i^t - state of the i^{th} cell in a particular time step t.
The model operates within a CA space composed of regular square cells interacting with each other within the Moore neighbourhood. The CA model was implemented in the object-oriented c++ programming language as an in-house code.

Models of Grain Boundary Curvature

As mentioned, the role of the P_{GB} during the growth of the grains under recrystallization conditions is evaluated in the current paper. For that, the different grain boundary curvature models are investigated (Fig. 1).

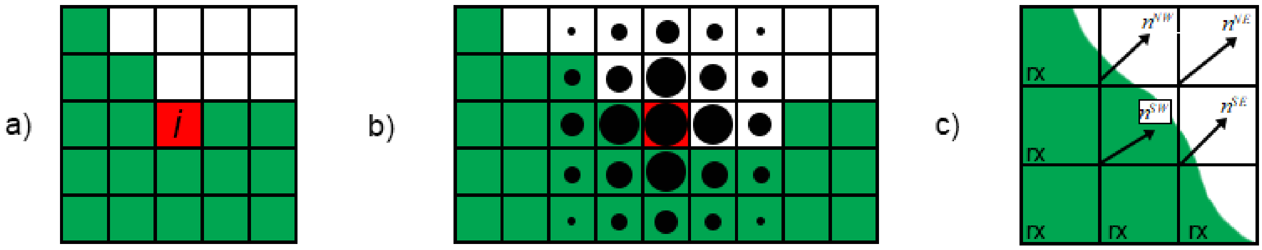

Fig. 1 Different models dedicated to the description of grain boundary curvature a) Kremeyer, b) Mason, c) concentration gradients.

The first is the standard Kremeyer model [17]. In this case, the grain boundary curvature value is determined based on the CA cells states within the extended Moore neighbourhood (Fig. 1a) and is expressed by the following formula:

$$\kappa = \frac{A}{a}\frac{Kink - N_i}{N+1} \tag{6}$$

where: a - the side length of the cell in the CA model, N - the sum of the number of neighbours of a given cell, N_i - the number of neighbouring cells that belong to the same grain as the considered cell, A - the aspect ratio depending on the cell shape (rectangular or hexagonal), $Kink$ - a constant equal to 15 for 2D space and 75 for 3D space, respectively.

The second investigated model is also based on the CA cell counting method and was proposed by Mason [18]. However, this model takes into account the interaction strength of neighbours. The closer the neighbour is to the interface cell, the stronger the interaction force (Fig. 1b). The interaction force between the two CA cells in a neighbourhood is calculated as:

$$F_{ij} = \exp\left[-\frac{\left(x_j - x_i\right)^2 + \left(y_j - y_i\right)^2}{2\sigma^2}\right] \tag{7}$$

where: σ - the standard deviation expressed in m, x and y - the cell coordinates in the global system of the cellular automaton space.
The effect of all neighbours on the central CA cell is calculated from the formula:

$$D = \sum_{j:F_{ij}\in S_i} F_{ij}\left(2\delta_{q_i q_j} - 1\right) \tag{8}$$

where: δ_{qiqj} - the Kronecker delta, q_i, q_j - variables that determine the affiliation of cells i and j, respectively, with a given grain, S_i - the set of all CA cells involved in the curvature calculation for cell i.

The calculation of grain curvature for a given cell in 2D space is performed using the following equation:

$$\kappa = \exp\left(\frac{\beta^2 a^2}{2\sigma^2}\right)\left[\frac{\alpha_P D}{\sqrt{2\pi}\sigma^3} - \frac{\sqrt{2\pi}}{\sigma} erf\left(\frac{\beta a}{\sqrt{2}\sigma}\right)\right] \tag{9}$$

where: β - the coefficient equal to 0.5 [23], α_p - the cell area expressed in m^2, a - the side length of the cell. According to the theoretical background of that model, the grain boundary must exist between adjacent cells, and the value of the calculated curvature has a unit of 1/m. In the Mason model, the σ parameter has to be identified as it may depend on the shape of the CA cells as well as the type of the neighbourhood [23].

The last investigated grain boundary model is called the concentration gradient model. It calculates the value of grain boundary curvature based on the fractional contribution of the phase volume fractions in the neighbourhood of the analysed CA cell. This model was originally proposed for the phase transformation simulations and is adapted in the current research to the SRX simulations. The method is based on the determination of the vertex normal to the transformation front using the differential method proposed in [24]. To determine the grain boundary curvature value, the coordinates of the normal vertex at each corner of the frontal CA cell are determined (Fig. 1c), and then the following relation is used:

$$\kappa = \frac{1}{\delta_{CA}}\left[\frac{\left(n_x^{SE} - n_x^{SW}\right) + \left(n_x^{NE} - n_x^{NW}\right)}{2} + \frac{\left(n_y^{NW} - n_y^{SW}\right) + \left(n_y^{NE} - n_y^{SE}\right)}{2}\right] \tag{10}$$

where: n_x^{SW}, n_x^{NW}, n_x^{NE}, n_x^{SE},n_y^{SW}, n_y^{NW},n_y^{NE}, n_y^{SE} - the coordinates of the normal versors at the corners of the CA cell under consideration. The four nearest CA cells surrounding a given corner and the value of the fraction of the recrystallized phase in each cell are used in the calculation of the vertex.

The coordinates of the normal versors $n = (n_x, n_y)$ are evaluated according to the following relations:

$$n_x = \frac{-\delta F_X}{\sqrt{(\delta F_X)^2 + (\delta F_Y)^2}} \qquad n_y = \frac{-\delta F_Y}{\sqrt{(\delta F_X)^2 + (\delta F_Y)^2}} \tag{11}$$

where:

$$\delta F_x = F\varphi^{NE} + F\varphi^{E} + F\varphi^{SE} - F\varphi^{NW} - F\varphi^{W} - F\varphi^{SW} \tag{12}$$

$$\delta F_y = F\varphi^{SW} + F\varphi^{S} + F\varphi^{SE} - F\varphi^{NW} - F\varphi^{N} - F\varphi^{NE} \tag{13}$$

The upper indices next to the symbols of the volume fractions $F\varphi$ refer to the geographical directions. The coordinates of the vertex located at the corner of the CA cell are calculated analogously, except that the corner is surrounded only by four neighbours, and only these neighbours are involved in evaluating the volume fraction δF_X and δF_X. The adapted concentration gradient model provides boundary curvature values that are much lower than the Kremeyer and Mason models, and that affects the grain growth velocity. The concentration gradient model does not have any parameter that can be used to influence the resulting boundary curvature value like the sigma parameter in the Mason model. Therefore, an additional model parameter ς was added to equation (10), which must also be identified for a given simulation setup. It should also be noted that the concentration gradient model is based on the differences in the recrystallized volume fractions within CA cells, and therefore it can not be applied to the simulation of grain growth after the end of recrystallization where all the CA cells are in the recrystallized state.

Results

The investigated static recrystallization simulation scenario takes into account the initial digital microstructure with 40 grains generated by the cellular automata unconstrained grain growth algorithm (Fig. 2a). Simulation and model parameters are set as follows: recrystallization temperature 1100 °C, dislocation density 8.8E14 1/m^2, SRX simulation time 20 s, CA time step 0.01 s, CA cell size 3E-7 m, heterogeneously distributed stored energy, site saturated nucleation with 81 nuclei. All the simulations are carried out until 50% of the recrystallized fraction to analyze the role of the grain boundary curvature during the course of static recrystallization. Three above-mentioned grain curvatures models: Kremeyer, Mason, and concentration gradient, are analyzed. The SRX simulation without any influence of the grain boundary curvature is considered as a reference result. As mentioned, both Mason and concentration gradient models have a parameter that can be modified for the simulations. For the Mason model, depending on the shape of the CA cell and the neighbourhood type, the typical value of σ varies between 1.19a and 3a [23]. However, Mason was also investigating higher values of sigma in his research [11]. Therefore, for the current investigation, five σ values were selected between 1a and 3a. The parameter ς (in the concentration gradient model) does not have any theoretical background, so the investigated values were selected arbitrarily based on the authors' experience from the range 1 - 20. Examples of obtained results for various analysed case studies are gathered in Fig. 2.

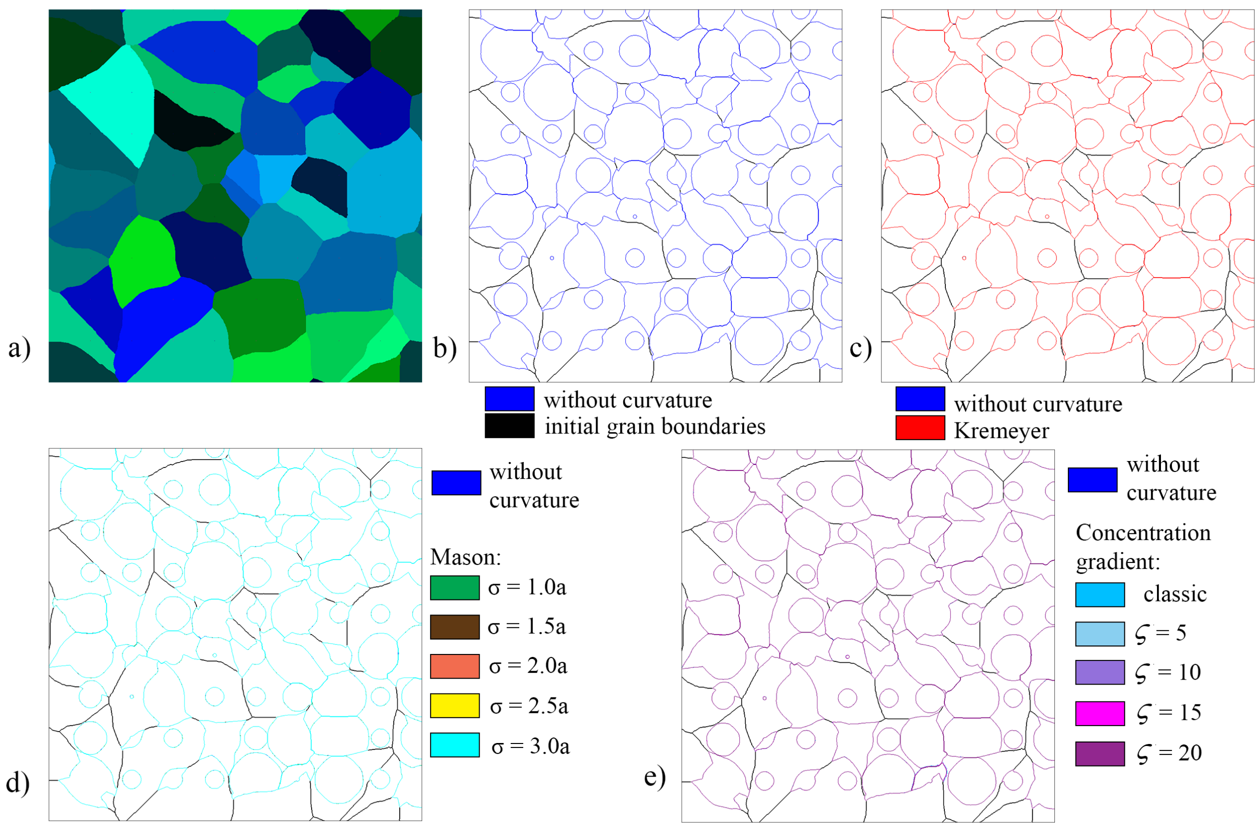

Fig. 2 a) initial digital microstructure prior SRX; b) reference 50% recrystallized microstructure without consideration of any curvature model; comparison of the model predictions for 50% recrystallization: c) without (blue) and with Kremeyer (red) curvature model, d) without (blue) and with Mason curvature model for various σ values (green - cyan) e) without (blue) and with concentration gradient curvature model for various ς values (deep blue - purple).

As presented in Fig. 2c-e, the grain boundary curvature models only slightly affect the growth of the grains under static recrystallization conditions. During the recrystallization, the grain boundary positions show minor differences in the order of single CA cells, which is presented in Fig. 3. This behaviour is because the driving force related to the grain boundary curvature seems to be negligible compared to the driving force associated with the stored energy. Even the high value of the scaling parameter in the concentration gradient model does not show a significant influence of the grain boundary curvature on the progress of static recrystallization. Therefore, based on these results, it can be concluded that the selection of the particular grain boundary curvature model for the static recrystallization simulations is not critical when the initial microstructure has, in general, equiaxed grains.

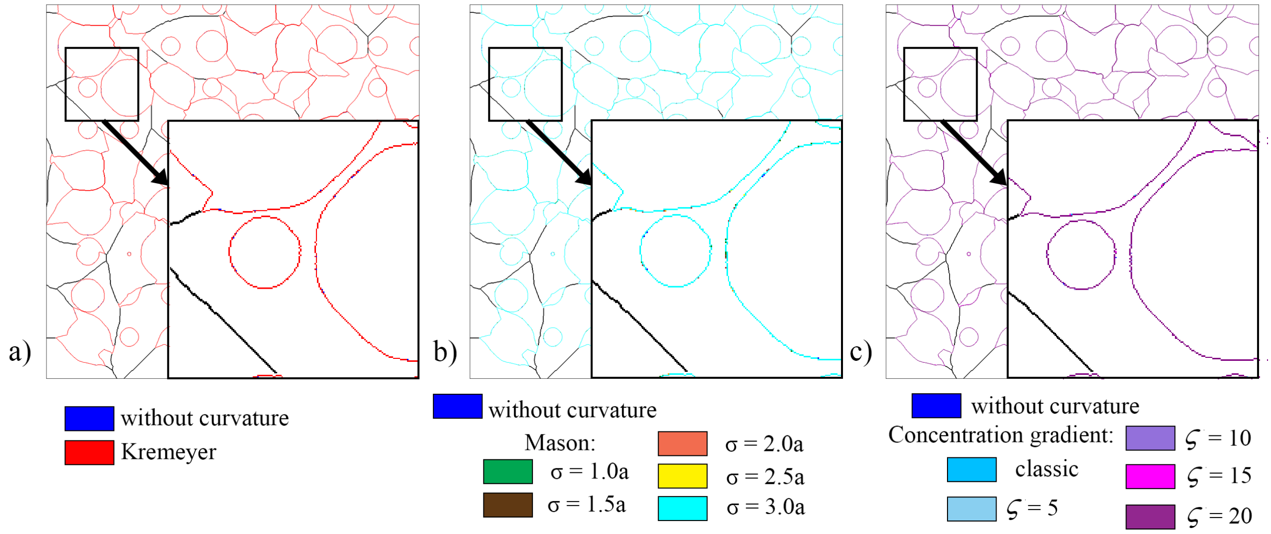

Fig. 3 The comparison of the model predictions for 50% recrystallization: c) without (blue) and with Kremeyer (red) curvature model, d) without (blue) and with Mason curvature model for various σ values (green - cyan) e) without (blue) and with concentration gradient curvature model for various ς values (green - cyan).

However, for further comparison, the research was additionally extended with the numerical simulation of the grain coarsening after the complete recrystallization. In this case, the driving force associated with the grain boundary curvature is the primary factor controlling grain growth. But at the same time, the role of the crystallographic orientation of grains on grain boundary mobility is also considered. For this set of simulations, the initial microstructure is obtained from the earlier investigation after 100% recrystallization, and the simulation time is extended to 300 s. As mentioned, the concentration gradient model cannot be used in this case, so the comparison is made only for the Kremeyer and Mason models. The state of the initial microstructure after recrystallization is shown in Fig. 4a, while grain growth simulation results for various models and their setups are in Fig. 4b - c.

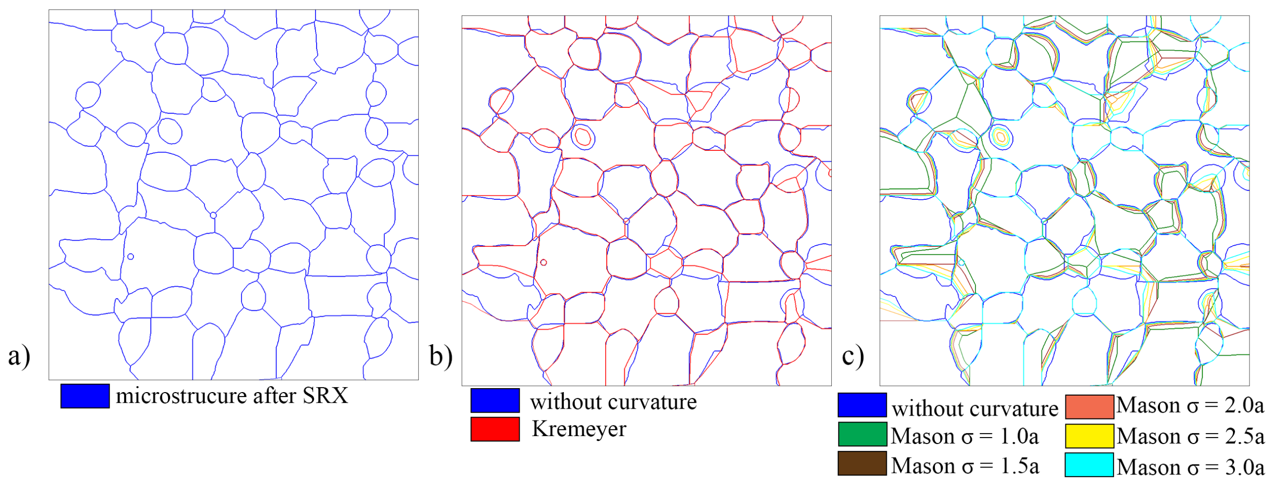

Fig. 4 a) Initial fully recrystallized microstructure; the comparison of the grain growth results without the influence of any curvature model (blue) and b) Kremeyer model (red) c) the Mason model for various σ values.

As presented, for the grain growth after the static recrystallization, the selection of the grain boundary curvature model starts to play a major role. In this case, the driving force associated with the grain boundary curvature is controlling the evolution of the grain boundaries. The Kremeyer model does not require any parameter identification prior to simulation and seems quite universal, making its application straightforward. The sigma value in the Masson model, on the other hand, has to be properly identified as its influence on the final results is significant.

Summary

Based on the presented research, several conclusions can be drawn:

- The selection of the particular grain boundary curvature model for the static recrystallization simulations is not critical. However, the current investigation was performed with a quite uniform initial microstructure with more or less equiaxed grains. The role of the grain boundary curvature models in the case of highly deformed microstructures, e.g., after 90% rolling reduction, still needs to be confirmed and will be the subject of future research.
- The grain boundary curvature model starts to play a role during the grain growth stages after the completion of the static recrystallization.
- The Kremeyer model seems quite universal, which makes its application straightforward both for static recrystallization and grain growth.
- The Mason model requires the identification of the σ parameter, especially for the grain growth stage. In general, smaller σ values favour grain growth.
- At this stage of research, the modified concentration gradient model is a simple approach that can be applied only to numerical simulation of grain boundary movement during static recrystallization. Further work will focus on extending its applicability to the grain growth simulations. Also, relating the scaling parameter to the size of the CA cell will be addressed.

Acknowledgement

Financial assistance of the National Science Centre project No. 2017/27/B/ST8/00373 is acknowledged.

References

[1] N. Haque, R.F. Cochrane, A.M. Mullis, Disorder-order morphologies in drop-tube processed Ni3Ge: Dendritic and seaweed growth, J. Alloys Compd. 707 (2017) 327–331. doi:10.1016/j.jallcom.2016.11.080.

[2] Y. Chen, Z. Hu, Y. Xu, J. Wang, P. Schützendübe, Y. Huang, Y. Liu, Z. Wang, Microstructure evolution and interface structure of Al-40 wt% Si composites produced by high-energy ball milling, J. Mater. Sci. Technol. 35 (2019) 512–519. doi:10.1016/j.jmst.2018.10.005.

[3] P. Lü, H.P. Wang, B. Wei, Competitive Nucleation and Growth Between the Primary and Peritectic Phases of Rapidly Solidifying Ni–Zr Hypoperitectic Alloy, Metall. Mater. Trans. A Phys. Metall. Mater. Sci. 50 (2019) 789–803. doi:10.1007/s11661-018-5048-7.

[4] L.Y. Zhao, H. Yan, R.S. Chen, E.H. Han, Study on the evolution pattern of grain orientation and misorientation during the static recrystallization of cold-rolled Mg-Zn-Gd alloy, Mater. Charact. 150 (2019) 252–266. doi:10.1016/j.matchar.2019.02.023.

[5] B.M. Patterson, K.C. Henderson, P.J. Gibbs, S.D. Imhoff, A.J. Clarke, Laboratory micro- and nanoscale X-ray tomographic investigation of Al-7 at.%Cu solidification structures, Mater. Charact. 95 (2014) 18–26. doi:10.1016/j.matchar.2014.06.004.

[6] H. Vafaeenezhad, S.H. Seyedein, M.R. Aboutalebi, A.R. Eivani, Hybrid Monte Carlo – Finite element simulation of microstructural evolution during annealing of severely deformed Sn-5Sb alloy, Comput. Mater. Sci. 163 (2019) 196–208. doi:10.1016/j.commatsci.2019.03.030.

[7] N. Maazi, B. Lezzar, An efficient Monte Carlo Potts method for the grain growth simulation of single-phase systems, Comput. Methods Mater. Sci. 20 (2020) 85–94. doi:10.7494/cmms.2020.3.0722.

[8] F. Roters, M. Diehl, P. Shanthraj, P. Eisenlohr, C. Reuber, S.L. Wong, T. Maiti, A. Ebrahimi, T. Hochrainer, H.O. Fabritius, S. Nikolov, M. Friák, N. Fujita, N. Grilli, K.G.F. Janssens, N. Jia, P.J.J. Kok, D. Ma, F. Meier, E. Werner, M. Stricker, D. Weygand, D. Raabe, DAMASK – The Düsseldorf Advanced Material Simulation Kit for modeling multi-physics crystal plasticity, thermal, and damage phenomena from the single crystal up to the component scale, Comput. Mater. Sci. 158 (2019) 420–478. doi:10.1016/j.commatsci.2018.04.030.

[9] S. Florez, M. Bernacki, A new fast and robust finite element strategy to simulate microstructural evolutions, Comput. Mater. Sci. 172 (2019) 109335. doi:10.1016/j.commatsci.2019.109335.

[10] K. Piekoś, J. Tarasiuk, K. Wierzbanowski, B. Bacroix, Stochastic vertex model of recrystallization, Comput. Mater. Sci. 42 (2008) 36–42. doi:10.1016/j.commatsci.2007.06.005.

[11] J.K. Mason, J. Lind, S.F. Li, B.W. Reed, M. Kumar, Kinetics and anisotropy of the Monte Carlo model of grain growth, Acta Mater. 82 (2015) 155–166. doi:10.1016/j.actamat.2014.08.063.

[12] C. Schwarze, R. Darvishi Kamachali, I. Steinbach, Phase-field study of zener drag and pinning of cylindrical particles in polycrystalline materials, Acta Mater. 106 (2016) 59–65. doi:10.1016/j.actamat.2015.10.045.

[13] D. Gurgul, W. Kapturkiewicz, A. Burbelko, Problem of the artificial anisotropy in solidification modeling by cellular automata method, Comput. Methods Mater. Sci. 7 (2007) 182–188.

[14] H.L. Ding, Y.Z. He, L.F. Liu, W.J. Ding, Cellular automata simulation of grain growth in three dimensions based on the lowest-energy principle, J. Cryst. Growth. 293 (2006) 489–497. doi:10.1016/j.jcrysgro.2006.05.060.

[15] S. Raghavan, S.S. Sahay, Modeling the grain growth kinetics by cellular automaton, Mater. Sci. Eng. A. 445–446 (2007) 203–209. doi:10.1016/j.msea.2006.09.023.

[16] Y. Vertyagina, M. Mahfouf, X. Xu, 3D modelling of ferrite and austenite grain coarsening using real-valued cellular automata based on transition function, J. Mater. Sci. 48 (2013) 5517–5527. doi:10.1007/s10853-013-7346-1.

[17] K. Kremeyer, Cellular Automata Investigations of Binary Solidification, J. Comput. Phys. 142 (1998) 243–263. doi:10.1006/jcph.1998.5926.

[18] J.K. Mason, Grain boundary energy and curvature in Monte Carlo and cellular automata simulations of grain boundary motion, Acta Mater. 94 (2015) 162–171. doi:10.1016/j.actamat.2015.04.047.

[19] D. Raabe, Recovery and Recrystallization: Phenomena, Physics, Models, Simulation, Fifth Edit, Elsevier, 2014. doi:10.1016/B978-0-444-53770-6.00023-X.

[20] R.L. Goetz, V. Seetharaman, Static Recrystallization Kinetics with Homogeneous and Heterogeneous Nucleation Using a Cellular Automata Model, Metall. Mater. Trans. A-Physical Metall. Mater. Sci. 29 (1998) 2307–2321. doi:10.1007/s11661-998-0108-z.

[21] L. Madej, L. Sieradzki, M. Sitko, K. Perzynski, K. Radwanski, R. Kuziak, Multi scale cellular automata and finite element based model for cold deformation and annealing of a ferritic-pearlitic microstructure, Comput. Mater. Sci. 77 (2013) 172–181. doi:10.1016/j.commatsci.2013.04.020.

[22] M. Sitko, Q. Chao, J. Wang, K. Perzynski, K. Muszka, L. Madej, A parallel version of the cellular automata static recrystallization model dedicated for high performance computing platforms – Development and verification, Comput. Mater. Sci. 172 (2020) 109283. doi:10.1016/j.commatsci.2019.109283.

[23] Z. Li, J. Wang, H. Huang, Grain boundary curvature based 2D cellular automata simulation of grain coarsening, J. Alloys Compd. 791 (2019) 411–422. doi:10.1016/j.jallcom.2019.03.195.

[24] M.J.M. Krane, D.R. Johnson, S. Raghavan, The development of a cellular automaton-finite volume model for dendritic growth, Appl. Math. Model. 33 (2009) 2234–2247. doi:10.1016/j.apm.2008.06.007.